Introgression from *Oryza meridionalis* into domesticated rice *Oryza sativa* results in shoot-based iron tolerance

Andriele Wairich[1], Ben Hur Neves de Oliveira[1], Lin-Bo Wu[2,3], Varunseelan Murugaiyan[2,4] Marcia Margis-Pinheiro[1,5], Janette Palma Fett[1,6], Felipe Klein Ricachenevsky[1,6], and Michael Frei[2]

[1]Programa de Pós-Graduação em Biologia Celular e Molecular, Centro de Biotecnologia, Universidade Federal do Rio Grande do Sul, Porto Alegre, Brazil.

[2]Institute for Crop Science and Resource Conservation (INRES), University of Bonn, Bonn, Germany.

[3]Institute for Molecular Physiology, Heinrich Heine University of Düsseldorf, Universitätsstraße 1, 40225 Düsseldorf, Germany

[4]Rice Breeding Platform, International Rice Research Institute (IRRI), Los Baños, Philippines.

[5]Departamento de Genética, Universidade Federal do Rio Grande do Sul, Porto Alegre, Brazil.

[6]Departamento de Botânica, Universidade Federal do Rio Grande do Sul, Porto Alegre, Brazil.

Andriele Wairich: andriwairich@gmail.com

Ben Hur Neves de Oliveira: oliveira.bhn@gmail.com

Lin-Bo Wu: wulinboyz@gmail.com

Varunseelan Murugaiyan: varunseelan@gmail.com

Marcia Margis-Pinheiro: marcia.margis@ufrgs.br

Janette Palma Fett: jpfett@cbiot.ufrgs.br

Felipe Klein Ricachenevsky: felipecruzalta@gmail.com

Michael Frei: mfrei@uni-bonn.de

Corresponding author: Dr. Michael Frei

Professor for Crop Science

University of Bonn - Institute of Crop Science and Resource Conservation, INRES

Katzenburgweg 5 13 53115 Bonn GERMANY

Tel.: +49 228 73-2881 FAX: +49-228-732489

Number of tables: 2

Number of figures: 7

Word count: 6432

Number of Supplementary Figures: 3

Number of Supplementary Tables: 8

Title, Highlight and Abstract

Introgression from *Oryza meridionalis* into domesticated rice *Oryza sativa* results in shoot-based iron tolerance

Short title

Iron tolerance of a wild rice hybrid

Highlight

We identified QTLs associated with iron tolerance derived from *O. meridionalis*, and characterized their physiological basis in *O. sativa*.

Abstract

Iron (Fe) toxicity is one of the most common mineral disorders affecting rice (*Oryza sativa*) production in flooded lowland fields. *Oryza meridionalis* is endemic from Northern Australia and grows in regions with Fe rich soils, making it a candidate for use in adaptive breeding. Aiming to understand tolerance mechanisms in rice, we screened a population of interspecific introgression lines (IL) from a cross between *O. sativa* and *O. meridionalis* for the identification of QTLs contributing to Fe toxicity tolerance. Six putative QTLs were identified. A line carrying one introgression from *O. meridionalis* on chromosome 9 associated with one QTL was highly tolerant despite very high shoot Fe concentrations. Physiological, biochemical, ionomic and transcriptomic analyses showed that the IL tolerance could partly be explained by Fe retention in the leaf sheath and culm. We constructed the interspecific hybrid genome *in silico* for transcriptomic analysis, and identified differentially regulated introgressed genes from *O. meridionalis* that could be involved in shoot-based Fe tolerance, such as metallothioneins, glutathione S-transferases and transporters from ABC and MFS families. This is the first work to demonstrate that introgressions of *O. meridionalis* into the *O. sativa* genome can confer increased tolerance to excess Fe.

Key Words and Abbreviations

Key Words: Crop wild relatives, metal toxicity, introgression line; hybrid genome; *Oryza sativa*; *Oryza meridionalis*; transcriptomics

Abbreviations:

+Fe: Fe toxicity

AAS: Atomic Absorption Spectrometry

CRI: carotenoid reflectance index

CSSL: chromosome segment substitution lines

DEG: differentially expressed gene

DW: dry weight

IL: introgression line

LB: leaf blades

LBS: leaf bronzing score

MDA: malondialdehyde

NDVI: normalized difference vegetation index

QTL: quantitative trait *loci*

RDVI: renormalized difference vegetation index

ROS: reactive oxygen species

RWR: rice wild relatives

TF: transcription factor

Introduction

Iron (Fe) is an essential microelement for almost all living organisms. In plants, Fe plays a critical role in respiration and photosynthesis and functions as a co-factor of many enzymes. However, when taken up excessively by plants, Fe becomes toxic as it participates in Fenton reactions catalyzing the generation of reactive oxygen species (ROS) (Guerinot and Yi, 1994). Fe toxicity (+Fe) is one of the most common mineral disorders affecting rice (*Oryza sativa* L.) production and yield in flooded lowland fields, where reducing conditions lead to excess availability of soluble ferrous iron (Becker and Asch, 2005, Fageria and Rabelo, 1987).

Fe toxicity symptoms include leaf bronzing, reduced tillering and poor development of roots, which become coated with a dark brown layer of Fe named Fe plaque (Becker and Asch, 2005, Audebert, 2006, Zhang *et al.*, 2016). However, different shoot or root-based mechanisms can confer tolerance to +Fe (Becker and Asch, 2005): (1) formation of root plaque through the precipitation of oxidized Fe(III), which acts as a physical barrier and prevents excessive Fe uptake; (2) retaining Fe in 'dumping sites', at which Fe is immobilized and deposited in a metabolically inactive form in root tissue (Becker and Asch, 2005, Audebert and Sahrawat, 2000); (3) shoot-based tolerance mechanism associated with the retention of Fe in less photosynthetically active tissues such as leaf sheath or culm, reducing the impact on photosynthesis; or on the storage of Fe excess in the apoplasm, vacuole and in plastids (by ferritin adsorption) (Engel *et al.*, 2012, Wu *et al.*, 2019, Silveira *et al.*, 2009); (4) control of Fenton-induced ROS formation by modulating plant redox homeostasis (Wu *et al.*, 2017).

Yield losses caused by +Fe usually range between 15% and 30%, but can reach the level of complete crop failure, depending on the intensity of the stress and plant age (Becker and Asch, 2005, Asch *et al.*, 2005). Strategies for mitigating yield losses include the selection of tolerant genotypes (Audebert, 2006). However, Fe tolerance is a quantitative trait controlled by multiple *loci* and genes. Moreover, the response of each specific genotype is dependent on its interaction with the environment (Dufey *et al.*, 2010, Wu *et al.*, 2014).

A significant constraint to the development of modern and high-yielding varieties is that the genetic diversity of the species *O. sativa* has been narrowed during rice domestication, and many traits associated with tolerance to adverse conditions (biotic or abiotic) may have been lost (Zhu *et al.*, 2007, Palmgren *et al.*, 2015, Menguer *et al.*, 2017). On the other hand, abundant natural variation in landraces and crop wild

120 relatives has been conserved in gene banks and constitutes a valuable genetic reservoir
121 that can be used for crop improvement. Thus rice wild relatives (RWR) have particular
122 importance as donors of genetic variation for cultivated rice (Arbelaez *et al.*, 2015,
123 Menguer *et al.*, 2017, Stein *et al.*, 2018).

124 Among RWR species, *O. meridionalis* is a promising source of tolerance to +Fe.
125 A screening of several genotypes representing 21 species of the genus *Oryza* for Fe
126 stress tolerance found two tolerant accessions of *O. meridionalis* (Bierschenk *et al.*,
127 2020). Tolerance to high Fe concentrations is likely related to the origin of the species,
128 which evolved in Northern Australia, at the edges of freshwater lagoons, seasonal
129 wetlands and swamps, in addition to Fe rich soils (Vaughan, 1994, Juliano *et al.*, 2005).
130 *O. meridionalis* is part of the primary gene pool (wild species closely related to *O.*
131 *sativa*), all containing AA genomes, which can cross breed for adaptive rice breeding
132 (Sotowa *et al.*, 2013, Bierschenk *et al.*, 2020).

133 This study aimed at deciphering interspecific genetic variation in adaptation to
134 +Fe and the underlying physiological mechanisms. This is a timely approach because
135 powerful resources for the exploitation of the global genetic diversity of the genus
136 *Oryza* have been developed recently, including populations derived from interspecific
137 crosses (Arbelaez *et al.*, 2015), as well as genome sequences of a variety of RWR
138 including *O. meridionalis* (Stein *et al.*, 2018). We used previously developed
139 introgression lines (IL) generated by crossing *O. sativa* and *O. meridionalis* and
140 screened it for tolerance to +Fe. Our specific hypotheses were (i) novel tolerance QTL
141 for +Fe can be identified by crossing the species barrier of *O. sativa;* (ii) *O.*
142 *meridionalis* introgressions can contribute novel adaptive traits that have not previously
143 been described in *O. sativa;* and (iii) transcriptome analyses using an *in silico*
144 constructed hybrid genome can shed light on the mechanisms underlying tolerance in an
145 interspecific hybrid.

146

147 **Materials and Methods**

148 **Plant material and screening for +Fe tolerance**

149 A population of 32 interspecific ILs was used in a screening for tolerance to
150 +Fe, which was generated from crosses between *O. sativa* cv Curinga (hereafter "*O.*
151 *sativa*") and *O. meridionalis* Ng. accession W2112 (Arbelaez *et al.*, 2015). Seeds were

originally obtained from Prof. Susan McCouch (Department of Plant Breeding and Genetics, Cornell University).

Experiments were conducted in a climate-controlled greenhouse in Bonn, Germany, from July to September 2018 (1st experiment) and from March to May 2019 (2nd experiment). Natural light was supplemented with artificial light between 7 am and 9 pm to ensure a minimum photosynthetic photon flux density of 400 µmol m^{-2} s^{-1}. The minimum day/night temperature was set to 28/22 ºC. Seeds were exposed to 55 ºC for three days to break dormancy. Seeds were germinated and seedlings were grown in a mesh floating on solutions containing 0.5 mM $CaCl_2$ and 10 µM $FeCl_3$ for two weeks at 28 ºC. The solutions were replaced twice a week. Eight seedlings per genotype per treatment (n = 4) were transplanted into 60 L containers (totalizing 8 containers), each containing 40 seedlings, filled with quarter-strength nutrient solution (Yoshida *et al.*, 1976). After one week, nutrient solutions were changed to half-strength, and thereafter replaced with a full-strength solution once a week (Wu *et al.*, 2019). The pH was adjusted to 5.5 every two days.

After three weeks of growth, plants were exposed to 250 mg L^{-1} of Fe as $FeSO_4.7H_2O$ for fifteen days. Nitrogen gas was percolated into the culture solutions for 15 minutes every 4 hours. The reflectance between 380 - 1050 nm of the three last fully expanded leaves was determined after 1, 3, 5, 7 and 13 days after the onset of treatment, with PolyPen RP 410 (Photon Systems Instruments Drasov, Czech Republic). Leaf bronzing scores (LBS) were attributed to the three youngest fully expanded leaves of the main tiller (Wu *et al.*, 2014), after 7 and 13 days of treatment. Plant material was harvested fifteen days after the onset of the experiment. The reduction of shoot and root growth were calculated as relative shoot/root dry weight (DW) = (shoot/root DW in treatment) / (shoot/root DW in the control). The concentration of Fe in shoots was quantified.

QTL mapping and statistical analysis

Chromosome segment substitution lines (CSSL) maps were constructed using SSR markers, and SNP-markers from 6K Infinium platform and GBS platform (Arbelaez *et al.*, 2015). Stepwise regression was used to select the most important segments for the traits evaluated and the likelihood ratio based on linear regression was used to estimate LOD scores. A permutation test using 1,000 permutations was carried out to determine the experiment-wise significance threshold (p = 0.05) and QTL

186 detection was completed using RSTEP-LRT-ADD method in CSL program of QTL
187 IciMapping v. 4.1 (Meng *et al.*, 2015), according to (Arbelaez *et al.*, 2015).
188
189 **Gas exchange measurements**
190 Gas exchange was measured with a portable photosynthetic gas exchange
191 system Li-Cor 6400-XT (LI-COR, Inc., Lincoln, NE, USA) 8 and 13 days after the
192 onset of the treatment. The youngest fully-expanded leaf on the main tiller of each plant
193 was evaluated between 10 am to 4 pm. Reference CO_2 concentration, flow rate and PAR
194 were set up at 400 µmol mol^{-1}, 300 mmol s^{-1} and 1000 µmol m^{-2} s^{-1}, respectively. Two
195 plants of each genotype per replicate (n = 8) were used for the measurements in both
196 treatments.
197
198 **Leaf spectral reflectance measurement**
199 Leaf spectral reflectance was measured on the first and second fully-expanded
200 leaves (6 plants per container; 4 containers) 7 and 14 days after the onset of the
201 treatments. Normalized difference vegetation index (NDVI) was calculated as: NDVI =
202 $(R_{NIR} - R_{RED})/(R_{NIR} + R_{RED})$, where R represents the reflectance at a given wavelength
203 (Huang *et al.*, 2013). Renormalized difference vegetation index (RDVI) was calculated
204 as: RDVI = $\frac{(NIR-Red)}{\sqrt{(NIR+Red)}}$ (Roujean and Breon, 1995). The carotenoid reflectance index
205 (CRI) I and II were determined in order to estimate carotenoid concentration relative to
206 chlorophyll concentration and were calculated as CRI I = $\frac{1}{\rho 510} - \frac{1}{\rho 550}$; CRI II =
207 $\frac{1}{\rho 510} - \frac{1}{\rho 700}$ (Gitelson *et al.*, 2002).
208
209 **LBS measurement**
210 Leaf bronzing symptoms were scored on the two youngest fully expanded leaves
211 of the main tiller, on a scale from 0 (no symptoms) to 10 (dead leaf) (Wu *et al.*, 2014).
212 The scoring was performed after 7 and 14 days of treatment.
213
214 **ROS staining in leaves**
215 In-situ detection of ROS was conducted in the youngest fully expanded leaf as
216 described (Wu *et al.*, 2017). ROS formation was visualized as brown precipitation,
217 documented by a camera (EOS 1200D, Canon, Tokyo, Japan).

Electrolyte leakage

To evaluate the cell membrane damage (Bajji *et al.*, 2002), the youngest fully expanded leaf was cut into small pieces of approximately 2 cm, washed three times with distilled water and stored in tubes filled with 30 mL of milli-Q water. Electrical conductivity measurements were taken at the moment of the harvest (0 h - ECi), 3, 6, 18 and 24 hours after harvest (ECf). After 24 h, the samples were autoclaved and a final measurement was performed. The electrolyte leakage was calculated as: (ECf-ECi)/(ECt-ECi)×100.

Malondialdehyde assay

Malondialdehyde (MDA) was quantified as 2-thiobarbituric-responsive substances (Höller *et al.*, 2014). Absorbance was measured at 440, 532 and 600 nm with a microplate reader (Powerwave XS2, BioTek) as described in (Rakotoson *et al.*, 2019). Calculations of MDA concentrations included background corrections.

Extraction of the root plaque

The root plaque from fresh roots was extracted with cold dithionite-citrate-bicarbonate (Taylor and Crowder, 1983), with some modifications. Rice roots were detached, washed once with distilled water and immersed in a solution of 20 mL of 0.3 M $Na_3C_6H_5O_7 \cdot 2H_2O$, 2.5 mL of 1.0 M $NaHCO_3$ and 1.5 g of $Na_2S_2O_4$ at room temperature. The solution was collected and the roots washed 3 times with 25 mL of distilled water. The resulting solution was made to final volume (100 mL) with distilled water and the washed roots were prepared for Fe determination by Atomic Absorption Spectrometry (AAS, Perkin-ELMER 1100B, Überlingen, Germany). Root oxidizing power was calculated as the amount of Fe precipitated on the root surface per root DW.

Determination of iron content in different tissues

For the determination of Fe content in root and shoot, as well as the compartmentalization of Fe in shoot, leaf blades (LB) were separated from the sheath and culm (here referred as culm). Tissues were dried at 60 ºC for seven days. Dry samples were ground to fine powder followed by digestion with 65% HNO_3 in a microwave pressure digestion system (MARS6, CEM GmbH, Kamp-Lintfort,

Germany). After digestion, samples were diluted to a final volume of 20 mL with distilled water. Fe content was determined by AAS (Perkin-ELMER 1100B).

RNA extraction and transcriptomic analysis

Total RNA was extracted with peqGOLD RNA kit (Peqlab; Erlangen, Germany) following the manufacturers' instructions. The genomic DNA was removed with RNAase-free with DNAase. The integrity of RNA was tested on a bleach agarose gel (Aranda *et al.*, 2012) and for purity using NanoDrop OneC (Thermo Fisher Scientific, Braunschweig, Germany).

For transcriptomic analysis, approximately 10 µg of total RNA was used for high-throughput cDNA sequencing by Illumina HiSeq^{TM} 4000 technology (BGI Genomics Co., Ltd – Denmark). RNAs derived from three biological replicates were used to generate the libraries. Eighteen libraries were constructed, from samples harvested seven days after the onset of treatments (control and +Fe). The cDNA libraries were prepared according to Illumina's protocols. After sequencing, read quality was checked and all low-quality reads (PHRED value < 20) were removed.

Expression Analysis

Genomes and genomic annotation for both *O. sativa* and *O. meridionalis* were obtained from Ensembl plants (https://plants.ensembl.org/index.html). Libraries from *O. sativa* cv. Curinga were aligned against the *O. sativa* genome, libraries from *O. meridionalis* were aligned against the *O. meridionalis* genome and libraries from CM23 were aligned against an *in silico* inferred CM23 genome (described below). Alignments were done using STAR (Dobin *et al.*, 2013) on default settings and feature counting was performed with the *SummarizeOverlaps* function on Union mode from the *GenomicAlignments* (Lawrence *et al.*, 2013) package for R. Principal component analyses were performed to cluster samples based on read count for quality control purposes. Subsequent differential expression analysis were performed (+Fe *vs*. control) through the standard protocol from DESeq2 (Love *et al.*, 2014) package for R. Genes for which *q-value* < 0.05 were considered differentially expressed (DEG). The R package fgsea (Korotkevich and Sukhov, 2016) was applied to find Gene Ontology terms induced or repressed by the +Fe treatment (number of permutations = 10^5, *q-value* < 0.05). For cross-species comparisons of DEG, we built a one-to-one correspondence table between *O. sativa* and *O. meridionalis* genes based on homology

information from Ensembl plants database. When, for a given gene, the homology relationship between species was of the type "one-to-many", we selected the one with highest sequence alignment identity. Intersection diagrams of DEGs in different species were done with the R package upSetR (Conway *et al.*, 2017). The data is publicly available through the GEO database with accession number GSE151559.

CM23 hybrid genome reconstruction

CM23 genome is a result of hybridization of wild parental *O. meridionalis* (≈ 6.18%) with *O. sativa*, with three major introgressions on chromosomes 7, 9 and 10. Based on the approximated coordinates of those introgressions originated from *O. meridionalis* (Arbelaez *et al.*, 2015), we used sequence homology to model the CM23 genome and used transcriptomic data to support the model. Assuming the introgressed DNA has to be placed at a homologous genomic segment, we considered S_N and E_N to be the start and end points of a given introgression coordinate in a chromosome *N* and defined as *RefSeq* the sequence from *O. sativa* on chromosome *N* from S_N to E_N. Then we used the *NucMer* script from MUMMER (Kurtz *et al.*, 2004) to align the *RefSeq* against the entire chromosome *N* of *O. meridionalis* with set parameters *maxgap* = 500 and *mincluster* = 100. Afterward, we filtered out aligned blocks that were both shorter than 2000 bases and had less than 90% identity. This large alignment was used to infer the introgression sequence (*i.e.*, the *O. meridionalis* sequence that is homologous to the *RefSeq*).

We used RNAseq libraries from CM23, *O. sativa* and *O. meridionalis* to support our introgression prediction. Each library was mapped against both *O. sativa* and *O. meridionalis* genomes using STAR (Dobin *et al.*, 2013) on default settings. Next, for each annotated exon in each evaluated chromosome, we calculated its coverage on each mapping job using *bedtools* (Quinlan and Hall, 2010). Then, in order to visualize coverage profile over the exons, we plotted line graphs as follows. First, we ranked each exon by its start position coordinate in the chromosome, which we called indexed position. Then a coverage profile (CP) for each indexed position *i* was calculated as: $CP_i = \frac{\sum_{i=1}^{i+w-1} \rho_i}{i+w-1}$, where ρ_i is the mean coverage of the exon whose indexed position is *i*, and $w \in \mathbb{N}$ is an arbitrary window size that defines the graph line smoothness. We also defined dissimilarity distance *D* between two coverage profiles as $D_i = (CP1_i - CP2i)^2$.

In summary, we artificially built the CM23 genome model by taking the *O. sativa* genome as a template and then proceeded to substitute genomic segments where introgressions occurred. Such segments were inferred according to homology and transcriptomic library coverage.

Results

Introgression lines show variation in Fe tolerance and accumulation

In order to identify Fe tolerant lines in the *O. sativa* x *O. meridionalis* population (hereafter CM), three-week-old plants were exposed to +Fe for 15 days. A hundred and eighteen phenotypic traits were evaluated, including biomass and growth-related traits, symptom formation, Fe concentration in shoot and spectral reflectance indexes of leaves (Table S1). The population showed significantly reduced shoot and root length under +Fe (Fig. S1A-B). When evaluating the relative DW, we observed that only eight (for shoots) and two lines (for roots) had significant decreases when submitted to +Fe, respectively (Fig. S1C-D). Symptoms related to stress, evaluated by LBS, began to develop after seven days of treatment. Thirteen days after the onset of the treatment *O. meridionalis* showed the lowest LBS (LBS = 1.0). Among the ILs, CM24 and CM23 were the most tolerant genotypes (1.25 and 2.25, respectively) (Fig. S1E).

Shoot Fe concentration and LBS were positively correlated in the CM population (Fig. 1). Considering all the lines, shoot Fe concentration explained only 11% ($p = 0.05$) of the observed variation in LBS. When we removed one outlier value (CM23 - Fe in shoot = 7.09 mg g^{-1} DW), the R^2 value increased to 31.34% ($p < 0.0007$).

QTL analyses reveal regions associated with Fe tolerance

QTL analysis was performed to identify *loci* underlying the genetic variation of the evaluated phenotypic traits in the population. A stepwise regression analysis identified six different regions on chromosomes 1, 4 and 9 that were significantly associated with 15 different traits (LOD > 2.75) (Table 1). These putative QTLs explained from 16.5% (RDVI on day 7 – segment 1.1) up to 49% (RDVI on day 7 – segment 4.4) of phenotypic variability. The lines CM23 and CM24, which presented the lowest LBS while showing high Fe concentration in the shoot (Fig. 1), share a common introgression on chromosome 9, segment 9.4 (Arbelaez *et al.*, 2015). This segment was associated with LBS and explained 42% of phenotypic variability (Table 1). The detection of putative QTLs for different traits in similar regions/segments (for example,

segment 1.1, 4.4 and 9.4) suggests that these regions harbor genes involved in +Fe tolerance.

Based on the screening and QTL analysis, CM23 was the most tolerant line from the CM population despite very high shoot Fe concentration (Fig. 1). This line and the parental genotypes, *O. sativa* and *O. meridionalis*, were used in subsequent experiments for physiological, biochemical and molecular analyses.

Introgression line CM23 and *O. meridionalis* are more tolerant to high Fe than *O. sativa*

Based on LBS data *O. meridionalis* and CM23 were more tolerant to Fe excess than *O. sativa* after seven and fourteen days of treatment (Fig. 2A). All three genotypes showed similar growth reduction under +Fe compared to the plants in the control (Fig. 2B-E). CM23 showed less reduction compared with *O. sativa* (Fig. 2C-E).

Leaf spectral reflectance indexes were used to monitor stress. The wild parental had higher relative values of NDVI than *O. sativa* and CM23 (Fig. 2F). Carotenoids are associated with light absorption in plants, and protect them from photo-oxidation. Stressed plants contain higher concentrations of carotenoids (Gitelson *et al.*, 2002). Consistently, Fe treatment significantly increased the CRI I and II in *O. meridionalis* after seven days of treatment (Fig. S2A-B). However, the relative values detected in CM23 for these same parameters were always below/near to 1, indicating lower concentrations of carotenoids accumulated in this IL (Fig. S2A-B).

Changes caused by +Fe on photosynthesis in all the three lines were investigated by gas exchange analysis. We found that the net photosynthetic rate in all three genotypes was clearly affected by Fe treatment, with negative values in CM23 starting after eight days under +Fe (Fig. S3A-B). Stomatal conductance and leaf transpiration rate were also significantly affected by the Fe treatment in all three genotypes (Fig. S3C-D). However, the relative values of CM23 were significantly higher than in both parents, indicating that it maintains higher transpiration and conductance under +Fe.

CM23 and *O. meridionalis* show lower oxidative stress under Fe stress

Seven days after the onset of the treatment, MDA concentration significantly increased in all genotypes when submitted to +Fe compared to control (Fig. 3A). *O. meridionalis* showed lower MDA concentration under +Fe compared to *O. sativa* and CM23 (Fig. 3A). After 14 days of +Fe, MDA increased in all genotypes compared to

controls (Fig. 3B). However, values were significantly higher in *O. sativa* compared to *O. meridionalis* and CM23. CM23 also showed the lowest electrolyte leakage value when compared with both parents, corroborating the tolerant character of this line (Fig. 3C).

DAB staining was employed to visualize H_2O_2 generation in leaves (Fig. 3D). In the control, no apparent differences in H_2O_2 staining were observed in *O. meridionalis*, *O. sativa* and CM23. With the exception of *O. meridionalis*, all genotypes had a small brown stains at the tip of the leaves, even in control. However, when plants were cultivated under +Fe, brown precipitates indicating H_2O_2 production were observed in the leaves of *O. sativa* (Fig. 3D), whereas lower levels were found in CM23, and even less was observed in *O. meridionalis*. These results indicate the high level of tolerance to Fe excess of *O. meridionalis* and CM23.

CM23 stores Fe in leaf sheaths and *O. meridionalis* excludes Fe from shoots

Fe concentration was analyzed in three different plant organs: LB, culm + sheath and roots. Fe treatment significantly increased Fe concentration in all shoot organs, as expected (Fig. 4A-B). No genotypic differences in Fe concentration in culm and sheath were observed under control. However, under +Fe, the highest Fe concentration in culm + sheath was observed in CM23 and lowest Fe concentration in the wild parent (Fig. 4A). The Fe concentration in the LB did not show any genotypic variation under control or +Fe treatment (Fig. 4B).

Only *O. sativa* and *O. meridionalis* responded with increased root Fe concentration under +Fe when compared with plants cultivated under control (Fig. 4C). CM23 had the lowest Fe concentration in roots, suggesting that the Fe absorbed by CM23 is translocated to shoot tissues. When the root oxidizing power was evaluated, only treatment differences were observed (Fig. 4D), suggesting that the tolerance presented by CM23 is based on a shoot mechanism.

Transcriptomic analysis of CM23 and parental lines under control and +Fe

Transcriptomic analyses were performed on shoots of *O. sativa*, *O. meridionalis* and CM23 plants exposed to control and +Fe conditions. A total of 4,171 genes (1,578 down and 2,593 up-regulated) were differentially expressed in *O. sativa*, accounting for 10.73% of all annotated genes (Table S2 and Fig. 5). In *O. meridionalis*, a total of 5,601 DEG (2,739 down and 2,862 up-regulated - Table S3 and Fig. 5) were identified (18.52

% of all annotated genes), whereas CM showed 1,449 (643 down and 806 up-regulated, with 27 and 47 introgressed genes, respectively) were DEG (3.78 % of all annotated genes) (Table S4 and Fig. 5).

When considering genes exclusively regulated in one genotype, we found 1,459, 1,852 and 240 exclusively up-regulated in *O. sativa*, *O. meridionalis* and CM23, respectively, and 886, 2,114 and 229 genes exclusively down-regulated (Fig. 5A-B and Tables S5 and S6). After the inference of homologies between *O. sativa* and *O. meridionalis*, we identified genes commonly regulated in different genotypes. A total of 687 and 370 DEG were up and down-regulated both in *O. sativa* and *O. meridionalis* respectively, 247 and 161 DEG up and down-regulated both in *O. sativa* and the IL CM23 respectively, and 123 and 94 DEG up and down-regulated both in *O. meridionalis* and CM23 respectively. However, when considering all genotypes, a total of 200 and 161 genes were up and down-regulated in common (Fig. 5A-B).

Gene set enrichment analysis (GSEA) of transcripts associated with +Fe response indicates similar processes regulated in all genotypes

Aiming to compare the transcriptomic changes in shoots under +Fe in *O. sativa*, *O. meridionalis* and CM23, we performed GSEA. We found 38 GO terms enriched in *O. sativa* (18 up and 20 down-regulated by +Fe), 31 GO terms enriched in *O. meridionalis* (16 up and 15 down-regulated) and 28 GO terms enriched in CM23 (16 up and 12 down-regulated) (Fig. 6 and 7).

Only three terms were overrepresented among up-regulated genes in all genotypes: “iron ion binding”, “monooxygenase activity” and “response to wounding” (Fig. 6A-C). On the other hand, two terms were overrepresented among down-regulated genes in all genotypes and both were associated with chloroplast: “chloroplast stroma” and “chloroplast envelope” (Fig. 7A-C).

Five terms were identified as equally overrepresented and up-regulated in *O. sativa* and *O. meridionalis*: “magnesium ion binding”, “terpene synthase activity”, “polysaccharide binding”, “recognition of pollen” and “lyase activity” (Fig. 6A-B). Two GO terms were commonly up-regulated between *O. sativa* and CM23: “chitinase activity” and “defense response”, suggesting a biotic stress response. *O. sativa* and CM23 did not share overrepresented GO terms for down-regulated genes.

Even though the number of GO terms up-regulated in CM23 was lower than in the parental genotypes, some of them were exclusively overrepresented: “transferase

activity, transferring hexosyl groups", "UDP−glycosyltransferase activity", and "intracellular membrane−bounded organelle" (Fig. 6C). On the other hand, the down-regulated terms exclusively overrepresented in CM23 followed the same pattern as those overrepresented the *O. meridionalis* ("photosystem II", "photosystem I", "plastoglobule", "chlorophyll biosynthetic process" and "ADP binding") (Fig. 7C).

Fe responsive genes in the tolerant CM23

In order to identify possible pathways and mechanisms linked to Fe tolerance in the interspecific hybrid, we focused on genes exclusively regulated in CM23 in comparison to the sensitive *O. sativa*. In contrast, we considered genes that were equally responsive to Fe stress in both the *O. sativa* parent and CM23 with a logFC >2 (Table S7) as stress response rather than stress tolerance genes.

We found that 377 genes were exclusively up-regulated in the tolerant CM23 (Table S8). These included a number of genes that could be involved in Fe homeostasis and detoxification, especially two genes encoding metallothionein genes (Os01g0200700, *OsMTI-3a* and Os05g0202800, *OsMTI-3b*). Another candidate would be an iron-responsive element-binding gene (Os08g0191100), which catalyzes the isomerization of citrate to isocitrate via cis-aconitate. Five transcription factors (TF) from the bHLH (basic helix-loop-helix) family, which has members involved in the regulation of Fe homeostasis (Gao *et al.*, 2019), were exclusively induced by +Fe in CM23. Also, a variety of transporters was contained in this list of genes, including potassium transporter OsHAK9 (Os07g0679000), high-affinity nitrate transporter OsNar2.2 (Os04g0480200), molybdate transporter OsMOT1 (Os08g0101500), copper transporter OsCOPT3 (Os03g0370800), and the sugar transport protein OsMST2 (Os03g0594400), which mediates active uptake of hexoses by sugar:proton symport. The heavy metal transport/detoxification protein (Os01g0976300) constitutes another plausible candidate that could be involved in Fe tolerance. Eight peroxidases were identified as induced by +Fe treatment in CM23 (Table S8), and could be involved in the removal of H_2O_2, oxidation of toxic reductants and general response to oxidative stress. We also identified several genes associated with osmotic stress and tolerance to salt and drought such as *Os-NADP-ME2* (Os01g0723400), *OsTIFY11a* (Os03g0180800), *OsMRS2* (Os01g0955100) and *OsMBL1* (Os01g0348900). These results suggest that osmoregulation could play a role in the tolerance to +Fe observed in CM23.

We further found that 332 genes exclusively down-regulated in CM23 compared to *O. sativa*. Among those were five TFs from the bHLH family and six TFs from the zinc finger family, as well as a gene from the WRKY family (*OsWRKY57* - Os12g0102300). Another category of downregulated genes in CM23 was transporters, including two genes from the oligopeptide transporter family, *OsOPT8* (Os02g0695800) and *OsOPT3* (Os06g0125500), one gene encoding a peptide transporter PTR2 (Os06g0239500), two genes from the ABC family transporters *OsABCG2* (Os01g0615500) and *OsABCC7* (Os04g0588700), and *OsNRAMP4* (Os01g0503400) (Table S8). In agreement with the data obtained from GSEA analysis, a great number of genes associated with photosynthesis such as genes coding for chlorophyll a/b-binding protein (Os02g0197600), ribulose bisphosphate carboxylase/oxygenase activase (Os04g0658300) and photosystem II stability/assembly factor HCF136 (Os06g0729650) were down-regulated under +Fe (Table S8). The same expression patterns was seen for the stay green-like protein (Os04g0692600), which promotes chlorophyll degradation in leaves (Rong *et al.*, 2013) was also down-regulated in CM23 by +Fe.

Fe-responsive genes introgressed from *O. meridionalis* into CM23

We further focused on genes that were both Fe-responsive and also located within the introgression segments of CM23. Out of 47 DEG introgressed from *O. meridionalis* and up-regulated by +Fe treatment, 20, 15 and 12 were located in the introgressions on chromosomes 7, 9 and 10, respectively. For eight out of these 47 genes, it was not possible to infer a homologue in *O. sativa*. From these eight *O. meridionalis*-specific genes, three are located on chromosome 7, three on chromosome 9 and two genes on chromosome 10 (Table 2).

Four genes similar to Glutathione S-transferase (GST) could play an important role in Fe tolerance, as GSTs are multifunctional enzymes contributing to cellular detoxification. Additional interesting genes that could be involved in Fe tolerance include one sugar/inositol transporter (OMERI07G01900/Os07g0151200); one putative hexose transporter (OMERI07G05590/Os07g0206600) that belongs to the major facilitator superfamily (MFS); one heavy metal transport/detoxification (OMERI10G13260); and the transporter urea-proton symporter DUR3 (OMERI10G14970) that plays an important role in high-affinity urea uptake by cells at low external urea concentrations (Wang *et al.*, 2012).

Genes encoding TFs from four different families were up-regulated (Table 2). The homeobox-leucine zipper protein HOX25 (OMERI09G06770) belongs to the HD-Zip I gene family of TF. The gene *OsSAP17* (OMERI09G06970 - zinc finger, AN1-type) encodes a protein with the A20/AN1 zinc-finger domain and plays a role in responses to abiotic stress (Vij and Tyagi, 2006). Other TFs identified are OMERI09G10200 which belongs to the APETALA2 (AP2)/Ethylene-Responsive Element Binding Factor family, and OMERI09G08730, similar to MYB TF family. Since TFs control the expression of numerous downstream genes providing stress tolerance to plants, these genes from *O. meridionalis* introgressed into CM23 genome could play essential roles in Fe tolerance.

From the introgression located on chromosome 9, we identified one ABC transporter-like domain containing protein - *ABCG47* (OMERI09G04710), and one gene coding for one acetylserotonin O-methyltransferase - *ASMT1* (OMERI09G05070) that is the final enzyme in a biosynthetic pathway that produces melatonin, which could provide protection against oxidative stress (Park *et al.*, 2013). Also, one CBL-interacting protein kinase 16 (OMERI09G08230), which has GO terms related to sodium ion transport and hyperosmotic salinity response, was also identified as induced by +Fe.

On the other hand, a total of 27 genes introgressed from *O. meridionalis* were down-regulated by +Fe treatment in CM23 (Table 2). Among these 27 genes, five genes located on chromosome 9 have no homologue in *O. sativa* genome (Table 2). In agreement with the GSEA analysis (Fig. 7) showing alterations on carbon metabolism, photosynthesis and photorespiration, a homologous gene associated with alanine aminotransferase metabolism in rice, *OsALT-2*, OMERI07G00150, for a gene described in *O. sativa* as “Ribose-5-phosphate isomerase precursor” (OMERI07G03430) and for a glycolate oxidase (EC 1.1.3.15) (OMERI07G02060) were introgressed from *O. meridionalis* and down-regulated by +Fe in CM23 (Table 2).

Discussion

Until now, no major locus conferring Fe excess tolerance has been fine-mapped or cloned (Meng *et al.*, 2017). Selection of Fe tolerant rice genotypes is difficult for two reasons: (1) the quantitative nature of the trait controlled by multiple small and medium effect loci (Wu *et al.*, 2014, Diop *et al.*, 2020); and (2) the narrowed genetic diversity of the domesticated *O. sativa* varieties (Jacquemin *et al.*, 2013, Menguer *et al.*, 2017). To overcome these limitations, ILs and CSSLs using RWR as donor parents can be useful (Arbelaez *et al.*, 2015, Bierschenk *et al.*, 2020). The use of a population of interspecific IL derived from crosses between *O. sativa* and *O. meridionalis* (Arbelaez *et al.*, 2015) was justified by previously reported tolerance of *O. meridionalis* accessions to Fe toxic conditions (Bierschenk *et al.*, 2020). This species' tolerance is probably associated with adaptation to its natural habitat in Northern Australia (Vaughan, 1994, Juliano *et al.*, 2005), a region characterized by wetlands and Fe rich soils (Cogle *et al.*, 2011). New QTLs were identified on chromosomes 1, 4, and 9 (Table 1). QTLs for LBS and relative decrease in shoot DW were also identified in different regions of chromosome 1 and 4 in previous studies (Wu *et al.*, 1997, Wu *et al.*, 1998, Dufey *et al.*, 2009, Quinet *et al.*, 2012, Wu *et al.*, 2014). However, this is the first report showing that Fe tolerance traits from *O. meridionalis* can be introgressed into *O. sativa*. Our results highlight the importance of ILs as a tool for genetic studies in interspecific crosses of rice (Guo and Ye, 2014, Arbelaez *et al.*, 2015).

Despite the fact that the *O. meridionalis* parent had low shoot Fe concentrations pointing to an exclusion mechanism, our physiological data suggested a shoot-based Fe tolerance mechanism in its progeny CM23. The interspecific hybrid exhibited high Fe storage in leaf sheaths and culms but less in the photosynthetically more active leaf blade (Fig. 4), a mechanism that was previously suggested to confer Fe tolerance (Audebert, 2006). Since translocation of Fe via the xylem follows the transpiration stream (Becker and Asch, 2005), the high Fe concentration in shoots of CM23 might be associated with the elevated transpiration rate of this genotype (Fig. S3D). CM23 also showed lower MDA levels compared to *O. sativa* (Fig. 3B-C), indicating that Fe is chelated or compartmentalized to avoid toxicity. Our previous work suggested shoot-based tolerance to +Fe in *O. sativa* can be achieved by modulating ascorbate recycling (Wu *et al.*, 2017), but we did not find indications that the same mechanisms operates in CM23 (data not shown). Taken together, our results demonstrate the importance of introgressed segments from *O. meridionalis* in shoot tolerance to +Fe. suggesting that

583 the *O. meridionalis* parent possesses novel shoot tolerance mechanisms in addition to its
584 Fe exclusion capacity and pyramids these complementary tolerance mechanisms.
585 Several studies reported the regulation of genes in response to Fe deficiency in
586 cultivated and wild rice (Ishimaru *et al.*, 2009, Zheng *et al.*, 2009, Bashir *et al.*, 2014,
587 Wairich *et al.*, 2019), while others have explored mechanism and genes regulated by
588 excess Fe (Quinet *et al.*, 2012, Bashir *et al.*, 2014, Stein *et al.*, 2019). However, to the
589 best of our knowledge, this is the first study to explore transcriptional responses of a
590 wild rice hybrid and its parents to Fe toxicity. Since the genome of CM23 has not been
591 sequenced, we reconstructed the interspecific hybrid genome *in silico* to map the
592 sequences from the transcriptomic analysis. This approach illustrated that the CM23
593 transcriptome was less responsive to Fe compared to the parents, and functional
594 categorization of DEGs showed striking differences (Fig. 6 and 7). Given the increasing
595 importance of crop wild relatives as sources of novel traits for agricultural crops
596 (Castaneda-Alvarez et al., 2016), we suggest that our methodological approach might be
597 useful for other similar studies investigating transcriptomic regulation in crops and their
598 wild relatives.
599 The plausibility of our transcriptome data is confirmed by the regulation of well
600 characterized Fe-responsive genes. Two rice ferritin genes (*OsFER1* and *OsFER2*) were
601 up-regulated in *O. sativa* and CM23 under +Fe. Ferritins are important proteins storing
602 Fe within the cell, and their accumulation has been shown in rice (Silveira *et al.*, 2009,
603 Stein et al 2009), maize (Briat *et al.*, 2010) and Arabidopsis (Tarantino *et al.*, 2010) in
604 response to Fe overload. In addition, VIT-like genes, Os04g0538400 and OsVIT2
605 (Os09g0396900), involved in the transport of Fe across the tonoplast (Zhang *et al.*,
606 2012) were up-regulated under Fe stress. These genes were also differentially regulated
607 in similar previous experiments in cultivated rice (Quinet *et al.*, 2012, Aung *et al.*, 2018,
608 Stein *et al.*, 2019). We also identified well-characterized genes involved in Fe-
609 homeostasis that were down-regulated in our dataset. *OsIRO2*, one of the positive
610 regulators of Fe deficiency response (Ogo *et al.*, 2006), was down-regulated in all
611 genotypes, suggesting all of them attempted to decrease Fe uptake. These data suggest
612 that these genes can be considered as marker genes for Fe toxicity stress.
613 However, the main purpose of this study was not to identify Fe responsive genes
614 but rather genes that may be involved in the shoot based tolerance mechanism of CM23,
615 such as genes exclusively differentially regulated in CM23. Although the number of
616 these genes was abundant, and it is possible that genes with hitherto unknown function

conferred tolerance, it is worthwhile discussing genes with an annotation related to metal homeostasis. Among those were two metallothionein-like proteins. These proteins buffer cytosolic metal concentration by the formation of mercaptide bonds between the metal and their numerous Cys residues (Kumar *et al.*, 2012).

Another category that could be of particular importance in conferring tolerance to CM23 are differentially regulated genes introgressed from *O. meridionalis* into CM23 (Table 8). Among those were GSTs, which are multifunctional enzymes playing a role in cellular detoxification (Salinas and Wong, 1999). In a previous microarray study, GSTs were also differentially regulated by +Fe in shoots of the tolerant *O. sativa* genotype FL483 compared to its more sensitive parent (Wu *et al.*, 2017). Here we found that four Fe-responsive GSTs from *O. meridionalis* introgressed into CM23 (one in chromosome 7 and three closely located genes in chromosome 10) were up-regulated in response to +Fe. Also, GSTs were previously suggested as candidate genes conferring tolerance to +Fe in genotypes of *O. sativa* in a genome wide association study (Matthus *et al.*, 2015). Within the chromosome 9 introgression segment, where our main QTL was located, only 15 genes were up-regulated by +Fe in CM23 (Table 2). Plausible candidate genes involved in +Fe response include also one ABC transporter (OMERI09G04710) and one MFS transporter (OMERI09G06320). ABC transporters were shown to detoxify As and Cd by transporting them into vacuoles (Zhang *et al.*, 2018, Fu *et al.*, 2019), whereas MFSs were involved in Fe homeostasis as transporters of nicotianamine and deoxymugineic acid (Che *et al.*, 2019, Haydon *et al.*, 2012). In order to confirm the involvement of these genes in Fe tolerance, further experiments would be required such as fine mapping and map-based cloning of QTL, or reverse genetic studies including genome editing. Overall our physiological and transcriptomic data suggest a shoot-based tolerance mechanism in the interspecific hybrid CM23, which is partly explained by retention of Fe in the leaf blade and culm, and could be regulated by genes involved in iron chelation, detoxification and partitioning.

In conclusion, our results highlight that RWR can be a rich reservoir of novel traits allowing plants to adapt to abiotic stress conditions. Introgressions from *O. meridionalis* conferred exceptional Fe tolerance to the interspecific hybrid line despite its very high shoot Fe concentrations. We further demonstrated that the availability of genome sequences for the wild relatives of crops form a powerful resource that allows for comparative transcriptional analyses of different species and crosses between them.

This approach provided us with plausible candidate genes involved in Fe tolerance originating from a RWR that remain to be explored further.

Supplementary data

Figure S1: Physiological parameters evaluated in the screening of 32 introgression lines under Fe excess (250 mg L^{-1} Fe^{2+}) after fifteen days of treatment

Figure S2: Relative carotenoid reflectance index I and II in plants of *O. sativa* cv. Curinga, *O. meridionalis* (Ng. acc. W2112) and CM23 exposed to Fe toxicity (250 mg L^{-1} Fe^{2+})

Figure S3: Responses of gas exchange in plants of *O. sativa* cv. Curinga, *O. meridionalis* (Ng. acc. W2112) and CM23 exposed to Fe toxicity (250 mg L^{-1} Fe^{2+} for 8 and 13 days)

Table S1: Traits evaluated in screening of CM population under Fe toxicity

Table S2: Transcriptome data sets with genes differentially expressed in shoots of *Oryza sativa* cv. Curinga after seven days under Fe excess (250 mg L^{-1} Fe^{2+})

Table S3: Transcriptome data sets with genes differentially expressed in shoots of *Oryza meridionalis* (Ng. acc. W2112) after seven days under Fe excess (250 mg L^{-1} Fe^{2+})

Table S4: Transcriptome data sets with genes differentially expressed in shoots of IL CM23 after seven days under Fe excess (250 mg L^{-1} Fe^{2+})

Table S5: Transcriptome data sets with homologue inferred genes commonly up-regulated in shoots of *O. sativa*, *O. meridionalis* and IL CM23 after seven days under Fe excess (250 mg L^{-1} Fe^{2+})

Table S6: Transcriptome data sets with homologue inferred genes commonly down-regulated in shoots of *O. sativa*, *O. meridionalis* and IL CM23 after seven days under Fe excess (250 mg L^{-1} Fe^{2+})

Table S7: Genes differentially expressed regulated commonly between CM23 and O. sativa cv. Curinga and logFC > 2.0 and logFC < 2.0

Table S8: Genes exclusively differentially expressed in CM23 (when compared with O. sativa cv. Curinga)

Acknowledgements

This study was financed in part by the Coordenação de Aperfeiçoamento de Pessoal de Nível Superior-Brasil (CAPES)-Finance Code 001 and Conselho Nacional de Desenvolvimento Científico e Tecnológico (CNPq), which granted fellowships to AW, BHNO, JPF, MMP and FKR. We also thank FAPERGS (Pronex process 16/25.51-

0000493-5) and CAPES/DAAD/Probral (process 88881.144076/2017-01). We also thank Prof. Susan McCouch for providing seeds of the interspecific introgression lines.

References

Audebert A. 2006. *Iron toxicity in rice-based systems in West Africa*. ADRAO, Cononou, Benin.

Aranda PS, LaJoie DM, Jorcyk CL. 2012. Bleach gel: a simple agarose gel for analyzing RNA quality. Electrophoresis **33**, 366–369.

Arbelaez JD, Moreno LT, Singh N, Tung CW, Maron LG, Ospina Y, Martinez CP, Grenier C, Lorieux M, McCouch S. 2015. Development and GBS-genotyping of introgression lines (ILs) using two wild species of rice, *O. meridionalis* and *O. rufipogon*, in a common recurrent parent, *O. sativa* cv. Curinga. Molecular Breeding **35**, 1–18.

Asch F, Becker M, Kpongor DS. 2005. A quick and efficient screen for resistance to iron toxicity in lowland rice. Journal of Plant Nutrition and Soil Science **168**, 764–773.

Audebert A, Sahrawat KL. 2000. Mechanisms for iron toxicity tolerance in lowland rice. Journal of Plant Nutrition **23**, 1877–1885.

Aung MS, Masuda H, Kobayashi T, Nishizawa NK. 2018. Physiological and transcriptomic analysis of responses to different levels of iron excess stress in various rice tissues. Soil Science and Plant Nutrition **64**, 370–385.

Bajji M, Kinet JM, Lutts S. 2002. The use of the electrolyte leakage method for assessing cell membrane stability as a water stress tolerance test in durum wheat. Plant Growth Regulation **36**, 61–70.

Bashir K, Hanada K, Shimizu M, Seki M, Nakanishi H, Nishizawa NK. 2014. Transcriptomic analysis of rice in response to iron deficiency and excess. Rice **7**, 1–15.

Becker M, Asch F. 2005. Iron toxicity in rice - conditions and management concepts. Journal of Plant Nutrition and Soil Science **168**, 558–573.

Bierschenk B, Tagele MT, Ali B, Ashrafuzzaman MD, Wu LB, Becker M, Frei M. 2020. Evaluation of rice wild relatives as a source of traits for adaptation to iron toxicity and enhanced grain quality. PLoS ONE **15**, 1–17.

Briat JF, Ravet K, Arnaud N, Duc C, Boucherez J, Touraine B, Cellier F, Gaymard F. 2010. New insights into ferritin synthesis and function highlight a link between iron homeostasis and oxidative stress in plants. Annals of Botany **105**, 811–822.

Castaneda-Alvarez NP, Khoury CK, Achicanoy HA, Bernau V, Dempewolf H, Eastwood RJ, Guarino L, Harker RH, Jarvis A, Maxted N, Müller JV, Ramirez-Villegas J, Sosa CC, Struik PC, Vincent H, Toll J. 2016. Global conservation priorities for crop wild relatives. Nature Plants **2,** 16022.

Che J, Yokosho K, Yamaji N, Ma JF. 2019. A vacuolar phytosiderophore transporter alters iron and zinc accumulation in polished rice grains. Plant Physiology **181**, 276–288.

Cogle AL, Keating MA, Langford PA, Gunton J, Webb IS. 2011. Runoff, soil loss, and nutrient transport from cropping systems on Red Ferrosols in tropical northern Australia. Soil Research **49**, 87–97.

Conway JR, Lex A, Gehlenborg N. 2017. UpSetR: an R package for the visualization of intersecting sets and their properties. Bioinformatics **33**, 2938–2940.

Diop B, Wang DR, Drame KN, Gracen V, Tongoona P, Dzidzienyo D, Nartey E, Greenberg AJ, Djida S, Danquah EY, McCouch SR. 2020. Brigding old and new: diversity and evaluation of high-iron associated stress response of rice cultivated in West Africa. Journal of Experimental Botany doi:10.1093/jxb/eraa182.

Dobin A, Davis CA, Schlesinger F, Drenkow J, Zaleski C, Jha S, Batut P, Chaisson M, Gingeras TR. 2013. STAR: Ultrafast universal RNA-seq aligner. Bioinformatics **29**, 15–21.

Dufey I, Hakizimana P, Draye X, Lutts S, Bertin P. 2009. QTL mapping for biomass and physiological parameters linked to resistance mechanisms to ferrous iron toxicity in rice. Euphytica **167**, 143–160.

Dufey I, Hiel MP, Hakizimana P, Draye X, Lutts S, Bertin P. 2010. Multi-environment QTL mapping and consistency across environments of resistance mechanisms to ferrous iron toxicity in rice. Second Africa Rice Congress, 1.10.1-1.10.15.

Engel K, Asch F, Becker M. 2012. Classification of rice genotypes based on their mechanisms of adaptation to iron toxicity. Journal of Plant Nutrition and Soil Science **175**, 871–881.

Fageria NK, Rabelo NA. 1987. Tolerance of rice cultivars to iron toxicity. Journal of Plant Nutrition **10**, 653–661.

Fu S, Lu Y, Zhang X, *et al.* 2019. The ABC transporter ABCG36 is required for cadmium tolerance in rice. Journal of Experimental Botany **70**, 5909–5918.

Gao F, Robe K, Gaymard F, Izquierdo E, Dubos C. 2019. The transcriptional control of iron homeostasis in plants: A tale of bHLH transcription factors? Frontiers in Plant Science **10**, 1–8.

Gitelson AA, Zur Y, Chivkunova OB, Merzlyak MN. 2002. Assessing carotenoid content in plant leaves with reflectance spectroscopy. Photochemistry and Photobiology **75**, 272–281.

Guerinot M Lou, Yi Y. 1994. Iron: nutritious, noxious, and not readily available. Plant Physiology **104**, 815–820.

Guo L, Ye G. 2014. Use of major quantitative trait loci to improve grain yield of rice. Rice Science **21**, 65–82.

Haydon MJ, Kawachi M, Wirtz M, Hillmer S, Hell R, Kramer U. 2012. Vacuolar nicotianamine has critical and distinct roles under iron deficiency and for zinc sequestration in Arabidopsis. the Plant Cell Online **24**, 724–737.

Höller S, Meyer A, Frei M. 2014. Zinc deficiency differentially affects redox homeostasis of rice genotypes contrasting in ascorbate level. Journal of Plant Physiology **171**, 1748–1756.

Huang J, Wang X, Li X, Tian H, Pan Z. 2013. Remotely sensed rice yield prediction using multi-temporal NDVI data derived from NOAA's-AVHRR. PLoS ONE **8**, 1–13.

Ishimaru Y, Bashir K, Fujimoto M, An G, Itai RN, Tsutsumi N, Nakanishi H, Nishizawa NK. 2009. Rice-specific *Mitochondrial Iron-Regulated* gene (*MIR*) plays an important role in iron homeostasis. Molecular Plant **2**, 1059–1066.

Jacquemin J, Bhatia D, Singh K, Wing RA. 2013. The international *Oryza* map alignment project: development of a genus-wide comparative genomics platform to help solve the 9 billion-people question. Current Opinion in Plant Biology **16**, 147–156.

Juliano AB, Naredo MEB, Lu BR, Jackson MT. 2005. Genetic differentiation in *Oryza meridionalis* Ng based on molecular and crossability analyses. Genetic Resources and Crop Evolution **52**, 435–445.

Korotkevich G, Sukhov V. 2016. Fast gene set enrichment analysis. bioRxiv, 1–29.

Kumar G, Kushwaha HR, Panjabi-Sabharwal V, Kumari S, Joshi R, Karan R, Mittal S, Singla-Pareek SL, Pareek A. 2012. Clustered metallothionein genes are co-regulated in rice and ectopic expression of *OsMT1e-P* confers multiple abiotic stress tolerance in tobacco via ROS scavenging. BMC Plant Biology **12**, 1–15.

Kurtz S, Phillippy A, Delcher AL, Smoot M, Shumway M, Antonescu C, Salzberg SL. 2004. Versatile and open software for comparing large genomes. Genome biology **5**, 12.1-12.9.

Lawrence M, Huber W, Pagès H, Aboyoun P, Carlson M, Gentleman R, Morgan MT, Carey VJ. 2013. Software for computing and annotating genomic ranges. PLoS Computational Biology **9**, 1–10.

Love MI, Huber W, Anders S. 2014. Moderated estimation of fold change and dispersion for RNA-seq data with DESeq2. Genome Biology **15**, 1–21.

Matthus E, Wu LB, Ueda Y, Höller S, Becker M, Frei M. 2015. Loci, genes, and mechanisms associated with tolerance to ferrous iron toxicity in rice (*Oryza sativa* L.). Theoretical and Applied Genetics **128**, 2085–2098.

Meng L, Li H, Zhang L, Wang J. 2015. QTL IciMapping: Integrated software for genetic linkage map construction and quantitative trait locus mapping in biparental populations. Crop Journal **3**, 269–283.

Meng L, Wang B, Zhao X, Ponce K, Qian Q, Ye G. 2017. Association mapping of ferrous, zinc, and aluminum tolerance at the seedling stage in indica rice using MAGIC populations. Frontiers in Plant Science **8**, 1–15.

Menguer PK, Sperotto RA, Ricachenevsky FK. 2017. A walk on the wild side: *Oryza* species as source for rice abiotic stress tolerance. Genetics and Molecular Biology **40**, 238–252.

Ogo Y, Itai RN, Nakanishi H, Inoue H, Kobayashi T, Suzuki M, Takahashi M, Mori S, Nishizawa NK. 2006. Isolation and characterization of *IRO2*, a novel iron-regulated bHLH transcription factor in graminaceous plants. Journal of Experimental Botany **57**, 2867–2878.

Palmgren MG, Edenbrandt AK, Vedel SE, *et al.* 2015. Are we ready for back-to-nature crop breeding? Trends in Plant Science **20**, 155–164.

Park S, Byeon Y, Back K. 2013. Functional analyses of three *ASMT* gene family members in rice plants. Journal of Pineal Research **55**, 409–415.

Quinet M, Vromman D, Clippe A, Bertin P, Lequeux H, Dufey I, Lutts S, Lefèvre I. 2012. Combined transcriptomic and physiological approaches reveal strong differences between short- and long-term response of rice (*Oryza sativa*) to iron toxicity. Plant, Cell and Environment **35**, 1837–1859.

Quinlan AR, Hall IM. 2010. BEDTools: A flexible suite of utilities for comparing genomic features. Bioinformatics **26**, 841–842.

Rakotoson T, Ergezinger L, Rajonandraina T, Razafimbelo T, Wu LB, Frei M. 2019. Physiological investigations of management and genotype options for adapting rice production to iron toxicity in Madagascar. Journal of Plant Nutrition and Soil Science **000**, 1–11.

Rong H, Tang Y, Zhang H, Wu P, Chen Y, Li M, Wu G, Jiang H. 2013. The *Stay-Green Rice Like* (*SGRL*) gene regulates chlorophyll degradation in rice. Journal of Plant Physiology **170**, 1367–1373.

Roujean JL, Breon FM. 1995. Estimating PAR absorbed by vegetation from bidirectional reflectance measurements. Remote Sensing of Environment **51**, 375–384.

Salinas AE, Wong MG. 1999. Glutathione S-transferases - a review. Current Medicinal Chemistry **6**, 279–309.

Silveira VC Da, Fadanelli C, Sperotto RA, Stein RJ, Basso LA, Santos DS, Vaz Junior IDS, Dias JF, Fett JP. 2009. Role of ferritin in the rice tolerance to iron overload. Scientia Agricola **66**, 549–555.

Sotowa M, Ootsuka K, Kobayashi Y, *et al.* 2013. Molecular relationships between Australian annual wild rice, *Oryza meridionalis*, and two related perennial forms. Rice **6**, 1–18.

Stein RJ, Duarte GL, Scheunemann L, Spohr MG, de Araújo Júnior AT, Ricachenevsky FK, Rosa LMG, Zanchin NIT, Santos RP dos, Fett JP. 2019. Genotype variation in rice (*Oryza sativa* L.) tolerance to Fe toxicity might be linked to root cell wall lignification. Frontiers in Plant Science **10**, 1–20.

Stein JC, Yu Y, Copetti D, *et al.* 2018. Genomes of 13 domesticated and wild rice relatives highlight genetic conservation, turnover and innovation across the genus *Oryza*. Nature Genetics **50**, 285–296.

Tarantino D, Santo N, Morandini P, Casagrande F, Braun H, Heinemeyer J, Vigani G, Soave C, Murgia I. 2010. *AtFer4* ferritin is a determinant of iron homeostasis in *Arabidopsis thaliana* heterotrophic cells. Journal of Plant Physiology **167**, 1598–1605.

Taylor GJ, Crowder AA. 1983. Use of the DCB technique for extraction of hydrous iron oxides from roots of wetland plants. American Journal of Botany **70**, 1254–1257.

Vaughan DA. 1994. *The wild relatives of rice: a genetic resources handbook.* Manila, Philippines: International Rice Research Institute.

Vij S, Tyagi AK. 2006. Genome-wide analysis of the *stress associated protein* (*SAP*) gene family containing A20/AN1 zinc-finger(s) in rice and their phylogenetic

relationship with Arabidopsis. Molecular Genetics and Genomics **276**, 565–575.

Wairich A, de Oliveira BHN, Arend EB, *et al.* 2019. The Combined Strategy for iron uptake is not exclusive to domesticated rice (*Oryza sativa*). Scientific Reports **9**, 1–17.

Wang WH, Köhler B, Cao FQ, *et al.* 2012. Rice *DUR3* mediates high-affinity urea transport and plays an effective role in improvement of urea acquisition and utilization when expressed in Arabidopsis. New Phytologist **193**, 432–444.

Wu L-B, Holtkamp F, Wairich A, Frei M. 2019. Potassium ion channel gene *OsAKT1* affects iron translocation in rice plants exposed to iron toxicity. Frontiers in Plant Science **10**, 1–14.

Wu P, Hu B, Liao CY, Zhu JM, Wu YR, Senadhira D, Paterson AH. 1998. Characterization of tissue tolerance to iron by molecular markers in different lines of rice. Plant and Soil **203**, 217–226.

Wu P, Luo A, Zhu J, Huang N, Senadhira D. 1997. Molecular markers linked to genes underlying seedling tolerance for ferrous iron toxicity. Plant Nutrition for sustainable food production and environment **64**, 789–792.

Wu LB, Shhadi MY, Gregorio G, Matthus E, Becker M, Frei M. 2014. Genetic and physiological analysis of tolerance to acute iron toxicity in rice. Rice **7**, 1–12.

Wu LB, Ueda Y, Lai SK, Frei M. 2017. Shoot tolerance mechanisms to iron toxicity in rice (*Oryza sativa* L.). Plant Cell and Environment **40**, 570–584.

Yoshida S, Forno AD, Cock JH, Gomez K a. 1976. Laboratory Manual for Physiological Studies of Rice. Dspaceirriorg, 69–72.

Zhang J, Martinoia E, Lee Y. 2018. Vacuolar transporters for cadmium and arsenic in plants and their applications in phytoremediation and crop development. Plant and Cell Physiology **59**, 1317–1325.

Zhang F, Xu T, Mao L, Yan S, Chen X, Wu Z, Chen R, Luo X, Xie J, Gao S. 2016. Genome-wide analysis of Dongxiang wild rice (*Oryza rufipogon* Griff.) to investigate lost/acquired genes during rice domestication. BMC Plant Biology **16**, 1–11.

Zhang Y, Xu YH, Yi HY, Gong JM. 2012. Vacuolar membrane transporters OsVIT1 and OsVIT2 modulate iron translocation between flag leaves and seeds in rice. Plant Journal **72**, 400–410.

Zheng L, Huang F, Narsai R, *et al.* 2009. Physiological and transcriptome analysis of iron and phosphorus interaction in rice seedlings. Plant Physiology **151**, 262–274.

Zhu Q, Zheng X, Luo J, Gaut BS, Ge S. 2007. Multilocus analysis of nucleotide variation of *Oryza sativa* and its wild relatives: severe bottleneck during domestication of rice. Molecular Biology and Evolution **24**, 875–888.

888 Table 1: Significant regions associated with traits evaluated during the screening of the
889 population *O. sativa* cv. Curinga x *O. meridionalis* (Ng. acc. W2112) (LOD > 2.75)
890 using a stepwise regression single marker analysis.

Trait name	Chr	Segment	Marker position (bp)	LOD	PVE(%)	Add
OSAVId7	1	1.1	3088667	6.1	27.5	0.0355
TVId7	1	1.1	3088667	4.0	23.5	0.0475
Lic1d7	1	1.1	3088667	5.2	24.7	0.0299
SIPId7	1	1.1	3088667	5.2	26.2	0.025
RDVId7	1	1.1	717702	3.5	16.6	0.0325
Gd5	4	4.4	18320014	2.8	34.1	-0.0598
NDVId7	4	4.4	18320014	2.8	31.5	-0.0483
OSAVId7	4	4.4	18320014	8.4	45.4	-0.0518
TVId7	4	4.4	18320014	5.3	35.0	-0.066
Lic1d7	4	4.4	18320014	7.7	44.9	-0.0457
SIPId7	4	4.4	18320014	7.1	41.5	-0.0357
RDVId7	4	4.4	18320014	7.5	48.7	-0.0558
CRI1d7	9	9.2	9195305	3.2	35.9	-0.0507
Lic2d7	9	9.3	12154616	3.1	37.8	-0.0715
LBS13	9	9.4	17948535	4.0	41.9	1.8188
Lic2d5	9	9.4	17948535	3.0	34.2	-0.0625
PRId7	9	9.4	17948535	3.0	33.6	-0.1578
ZMId13	9	9.4	19065062	2.7	31.7	-0.0602
Lic2d13	9	9.4	19065062	3.5	39.5	-0.0902
GM1d13	9	9.5	21802016	3.7	39.4	-0.0763

891 Chr: chromosome; LOD: logarithm of odds; PVE: phenotypic variability explained;
892 Add: additive effect; OSAVI: Optimized Soil-Adjusted Vegetation Index; TVI:
893 Triangular Vegetation Index; Lic1 and Lic2: Lichtenthaler Indexes; SIPI: Structure
894 Intensive Pigment Index; RDVI: Renormalized Difference Vegetation Index; G:
895 Greenness Index; NDVI: Normalized Difference Vegetation Index; CRI1: Carotenoid
896 Reflectance Index 1; LBS: leaf bronzing score; PRI: Photochemical Reflectance Index;
897 ZMI: Zarco-Tejada & Miller Index; GMI: Gitelson and Merzlyak Index; d indicates the
898 day after the start of the treatment.
899

900 Table 2: Differentially expressed genes introgressed from *O. meridionalis* into CM23.

Gene_ID	logFC	q value	Homologous gene	Description homologous
		Up-regulated genes		
OMERI07G00330	1.065	0.0097	Os07g0114000	Similar to Protein phosphatase 2C-like
OMERI07G00620	1.848	0.005	-	-
OMERI07G01050	1.588	0.032	Os07g0127500	Similar to PR-1a pathogenesis related protein (Hv-1a) precursor
OMERI07G01070	1.647	0.020	-	-
OMERI07G01130	3.062	6.72E-15	-	-
OMERI07G01900	0.733	0.044	Os07g0151200	Sugar/inositol transporter domain containing protein
OMERI07G02190	1.114	0.00014	Os07g0158800	Protein of unknown function DUF266, plant family protein
OMERI07G02920	1.530	0.008	Os07g0168300	Similar to Glutathione S-transferase GSTU6
OMERI07G02960	1.611	3.23E-5	Os07g0170000	Similar to Brn1-like protein
OMERI07G03280	1.219	0.011	Os07g0174400	Similar to Non-specific lipid-transfer protein
OMERI07G03370	1.462	0.002	Os07g0175600	Plant lipid transfer protein and hydrophobic protein, helical domain containing protein
OMERI07G04020	1.141	0.002	Os07g0192000	ATPase, AAA-type, core domain containing protein
OMERI07G05270	1.682	8.07E-9	Os07g0201800	UDP-glucuronosyl/UDP-glucosyltransferase domain containing protein
OMERI07G05590	0.716	0.005	Os07g0206600	Similar to Hexose transporter
OMERI07G06160	4.076	3.51E-12	Os07G0218700	Cytochrome P450 family protein
OMERI07G06460	1.383	0.005	Os07g0231800	Conserved hypothetical protein
OMERI07G06790	2.340	0.002	Os08g0412700	Protein of unknown function DUF1262 family protein
OMERI07G06870	1.404	0.0001	Os07g0241800	UDP-glucuronosyl/UDP-glucosyltransferase family protein
OMERI07G07720	0.874	0.039	Os10g0566400	Similar to RING-H2 finger protein ATL3J
OMERI09G04710	2.031	0.021	Os09g0333000	ABC transporter-like domain containing protein
OMERI09G05070	2.420	7.369E-6	Os09g0344500	Similar to O-methyltransferase ZRP4 (EC 2.1.1.)
OMERI09G06280	1.064	0.001	Os09g0370500	VQ domain containing protein
OMERI09G06320	1.162	0.012	Os09g0371300	Similar to predicted protein
OMERI09G06770	1.465	0.001	Os09g0379600	Similar to Homeobox-leucine zipper protein HOX25
OMERI09G06970	1.368	0.001	Os09g0385700	Zinc finger, AN1-type domain containing protein
OMERI09G07290	3.897	1.869E-7	-	-
OMERI09G07310	2.636	0.015	-	-
OMERI09G08230	1.155	0.005	Os09g0418000	Similar to CBL-interacting protein kinase 16
OMERI09G08730	1.167	0.017	Os09g0431300	Similar to MYB transcription factor MYB71 (Fragment)
OMERI09G09130	1.165	0.003	Os09g0439200	Jasmonate ZIM-domain protein, Jasmonate-induced resistance to bacterial blight, Repressor of jasmonic acid signalin
OMERI09G10000	1.856	0.007	Os09g0454600	Similar to Mitochondrial phosphate transporter (Fragment)
OMERI09G10200	2.953	0.033	Os09g0457900	AP2/ERF transcription factor, Regulation of the internode elongation
OMERI09G10280	1.385	0.028	Os08g0478466	Protein of unknown function DUF296 domain containing protein
OMERI09G10540	1.379	0.003		
OMERI10G12860	1.116	0.017	Os10g0524300	LysM domain-containing protein, Embryo sac development
OMERI10G13020	2.167	1.33E-7	Os10g0527601	Glutathione S-transferase, C-terminal-like domain containing protein
OMERI10G13050	0.750	0.006	Os10g0529400	Similar to Glutathione S-transferase GSTU6

OMERI10G13130	1.584	3.86E-7	Os10g0530600	Similar to Glutathione S-transferase GST 20 (EC 2.5.1.18)
OMERI10G13260	1.337	0.027	Os10g0532300	Heavy metal transport/detoxification protein domain containing protein
OMERI10G13550	1.873	0.005		
OMERI10G13880	1.390	0.0004	Os10g0542800	Brassinosteroid-signaling kinase, A member of the receptor-like cytoplasmic kinase (RLCK)-XII sub group, Major regulator in rice immunit
OMERI10G14200	2.331	0.006	Os10g0548100	Similar to DM280 protein
OMERI10G14220	1.058	0.011	Os10g0548400	Similar to F25C20.9
OMERI10G14500	1.533	0.012		
OMERI10G14970	1.739	0.001	Os10g0580400	High-affinity urea transporter, Effective urea acquisition and utilisation, Effective use of low external urea as a N sourc
OMERI10G15240	1.098	6.36E-5	Os10g0576600	Tetratricopeptide-like helical domain containing protein
		Down-regulated genes		
OMERI07G00150	-1.192	0.0002	Os07g0108300	Similar to Alanine aminotransferase
OMERI07G00410	-0.864	0.026	Os07g0115300	Similar to Peroxidase2 precursor (EC 1.11.1.7)
OMERI07G01650	-0.825	0.030		
OMERI07G02060	-0.851	0.006	Os07g0152900	Similar to Glycolate oxidase (EC 1.1.3.15) (Fragment)
OMERI07G02290	-1.188	0.0009	Os07g0159700	Protein kinase, catalytic domain domain containing protein
OMERI07G02340	-0.857	0.035	Os07g0160400	Glyoxalase/bleomycin resistance protein/dioxygenase domain containing protein
OMERI07G03430	-0.660	0.048	Os07g0176900	Similar to Ribose-5-phosphate isomerase precursor (EC 5.3.1.6)
OMERI07G03910	-1.011	0.005	Os07g0191200	Plasma membrane H+ ATPase (EC 3.6.3.6)
OMERI07G05950	-1.080	0.0005	Os07g0212200	Similar to MRNA-binding protein (Fragment)
OMERI09G03920	-0.694	0.020	Os09g0307300	Targeting for Xklp2 family protein
OMERI09G04970	-1.204	0.010	Os09g0343200	Ankyrin repeat containing protein
OMERI09G05320	-4.16	1.48E-5	Os08g0327200	OsPGL4
OMERI09G05460	-1.982	6.77E-6	Os09g0350900	Protein kinase, core domain containing protein
OMERI09G05480	-4.369	6.39E-7		
OMERI09G05570	-2.252	5.49E-6		
OMERI09G06420	-1.704	0.017		
OMERI09G06460	-1.185	0.023		
OMERI09G07520	-0.860	0.015	Os09g0402300	Phosphatidylinositol-4-phosphate 5-kinase family protein
OMERI09G08870	-1.169	2.16E-5	Os09g0434500	Similar to Ethylene response factor 2
OMERI09G09840	-0.850	0.040	Os09g0452800	Peptidase A1 domain containing protein
OMERI09G10700	-0.904	0.013		
OMERI09G10710	-0.787	0.019	Os09g0477900	NusB/RsmB/TIM44 domain containing protein
OMERI10G13120	-1.279	0.0005	Os10g0530500	Similar to Glutathione-S-transferase Cla47
OMERI10G13320	-0.824	0.024	Os10g0533500	Similar to Beta-ring hydroxylase (Fragment)
OMERI10G13640	-0.917	0.028	Os10g0539900	Tonoplast monosaccharide transpoter, Vacuolar sugar transpor
OMERI10G14830	-0.923	0.003		
OMERI10G15060	-1.785	0.0004	Os10g0578950	Similar to 4-coumarate--CoA ligase-like 2

901

902 **Figure legends**

903 Figure 1: Linear regression of shoot Fe concentration *versus* leaf bronzing score (LBS)
904 in *O. sativa* cv. Curinga x *O. meridionalis* (Ng. acc. W2112) (CM) population
905 submitted to 250 mg L^{-1} of Fe for fifteen days. The dark blue data point represents the
906 sensitive parental, *O. sativa* cv. Curinga. The light blue data point represents the tolerant
907 parental *O. meridionalis* (Ng. acc. W2112). The pink data point represents the tolerant
908 line with low symptom formation and high Fe concentration on shoots, named CM 23.
909 The upper equation represents the values of correlation after the outlier value was
910 removed.
911
912 Figure 2: Responses of parents and selected introgression lines exposed to Fe toxicity
913 (250 mg L^{-1} Fe^{2+}) for 14 days. (A) Leaf bronzing score in Fe treatment after seven and
914 fourteen days of treatment (n = 16). (B) Relative shoot length (n = 16). (C) Relative root
915 length (n = 16). (D) Relative shoot dry weight (n = 16). (E) Relative root dry weight (n
916 = 16). Values are the averages ± SE. Asterisks indicate statistical difference when
917 compared with *O. sativa* (Student *t*-test, **P-value < 0.01). Different letters above the
918 bars indicate the differences were significant at $P < 0.05$ by *post hoc* Tukey's test.
919 Uppercase represents comparisons in seven days and lowercase comparisons between
920 fourteen days after onset of Fe toxicity. (F) Relative normalized difference vegetation
921 index (NDVI) on days 7 and 11 after the onset of treatment (n = 16). Different letters
922 above the bars indicate the differences were significant at $P < 0.05$ by *post hoc* Tukey's
923 test. Uppercase represents comparisons between genotypes after seven days and
924 lowercase comparisons between genotypes after eleven days of Fe excess treatment.
925
926 Figure 3: Physiological analysis of the tolerance to Fe toxicity. Shoot MDA
927 concentration in contrasting parents (*O. sativa* cv. Curinga and *O. meridionalis* (Ng.
928 acc. W2112) and in IL CM23 submitted to control and +Fe (250 mg L^{-1} Fe^{2+}). Plants
929 were submitted to +Fe for seven (A) and fourteen (B) days. (n = 4). Values are the
930 averages ± SE. Asterisks indicate statistical difference between control and +Fe
931 (Student *t*-test, ***P-value < 0.001). Different letters above the bars indicate the
932 differences were significant at $P < 0.05$ by *post hoc* Tukey's test. Uppercase represents
933 comparisons between genotypes in control and lowercase comparisons in Fe toxicity.
934 (C) Relative electrolyte leakage in leaves of parents and selected introgression line
935 (CM23) submitted to control condition and Fe toxicity for 14 days (n = 16). (Student *t*-

test, ***P-value < 0.001). (D) Hydrogen peroxide staining using 3,3′-Diaminobenzidine of parents and selected introgression line (CM23) under control and Fe toxicity (250 mg L^{-1} Fe^{2+} for 7 days) (n=4).

Figure 4: Fe concentration in three different organs of *O. sativa* cv. Curinga, *O. meridionalis* (Ng. acc. W2112) and in CM23 exposed to control conditions and to Fe toxicity (250 mg L^{-1} Fe^{2+}) for fourteen days. (A) Fe concentration in leaf sheath and culm (mg g^{-1} DW). (B) Fe concentration in leaf blades (mg g^{-1} DW). (C) Fe concentration in roots (mg g^{-1} DW). (D) Root oxidation power (Fe concentration in the iron plaque) (mg Fe g^{-1} DW). (n = 8). Values are the averages ± SE. Different letters above the bars indicate that the differences were significant at $P < 0.05$ by *post hoc* Tukey's test. Uppercase letters represent comparisons in control and lowercase comparisons between genotypes under Fe toxicity. Asterisks indicate statistical difference between plants grown under CC and +Fe conditions (Student *t*-test, ****P-value < 0.0001).

Figure 5: Upset chart with genes up and down-regulated by Fe toxicity (250 mg L^{-1} Fe^{2+}) seven days after + Fe treatment in *O. sativa* cv. Curinga, *O. meridionalis* (Ng. acc. W2112) and the IL CM23. (A) Genes up and (B) down-regulated by Fe treatment in *O. meridionalis*, *O. sativa* cv. Curinga, CM23, genes commonly regulated between *O. sativa* and *O. meridionalis*, *O. sativa* and CM23, *O. meridionalis* and CM23, and commonly regulated in all three genotypes. CUR: *O. sativa* cv. Curinga; MER: *O. meridionalis;* CM23: IL CM23.

Figure 6: Gene set enrichment analysis of up-regulated genes in the transcriptome of shoots from *O. sativa* cv. Curinga, *O. meridionalis* (Ng. acc. W2112) and IL CM23 seven days after the onset of treatment with Fe excess (250 mg L^{-1} Fe^{2+}). The line represents the genes ordered by logFC. The higher the logFC of a gene, the more to left the line corresponding to that gene is represented.

Figure 7: Gene set enrichment analysis of down-regulated genes on the transcriptome from shoots of *O. sativa* cv. Curinga, *O. meridionalis* (Ng. acc. W2112) and IL CM23 seven days after the onset of treatment with Fe excess (250 mg L^{-1} Fe^{2+}). The line

969 represents the genes ordered by logFC. The higher the logFC of a gene, the more to
970 right the line corresponding to that gene is represented.

971 Figure 1:

972

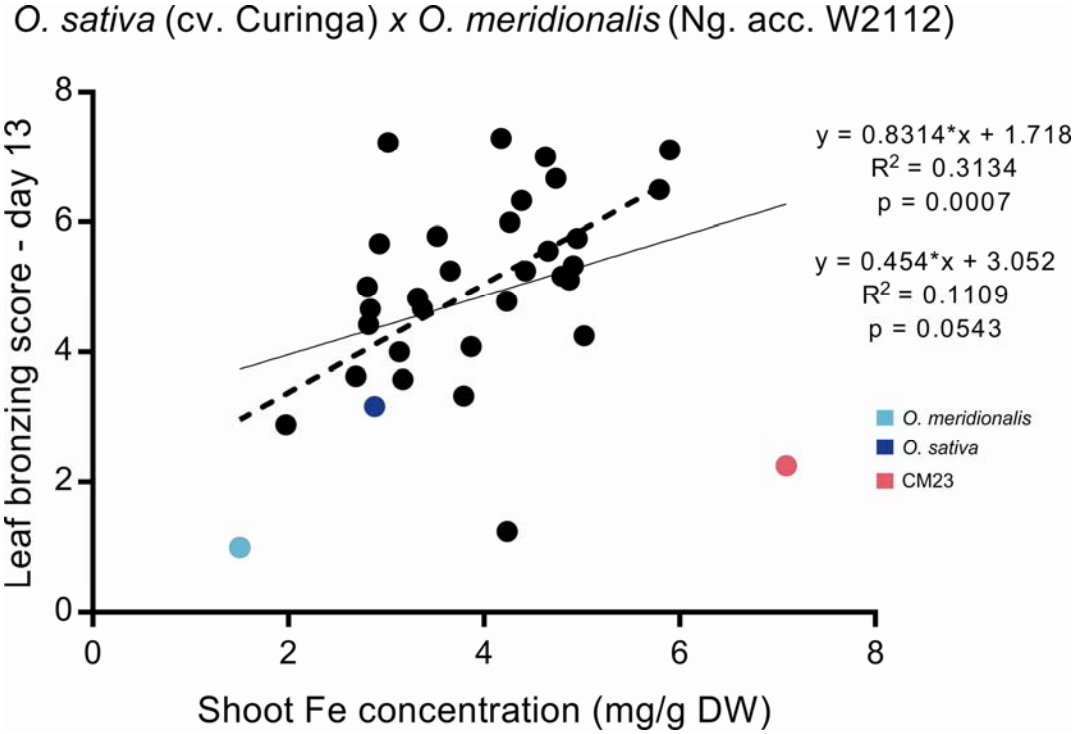

973

974

975 Figure 2

976

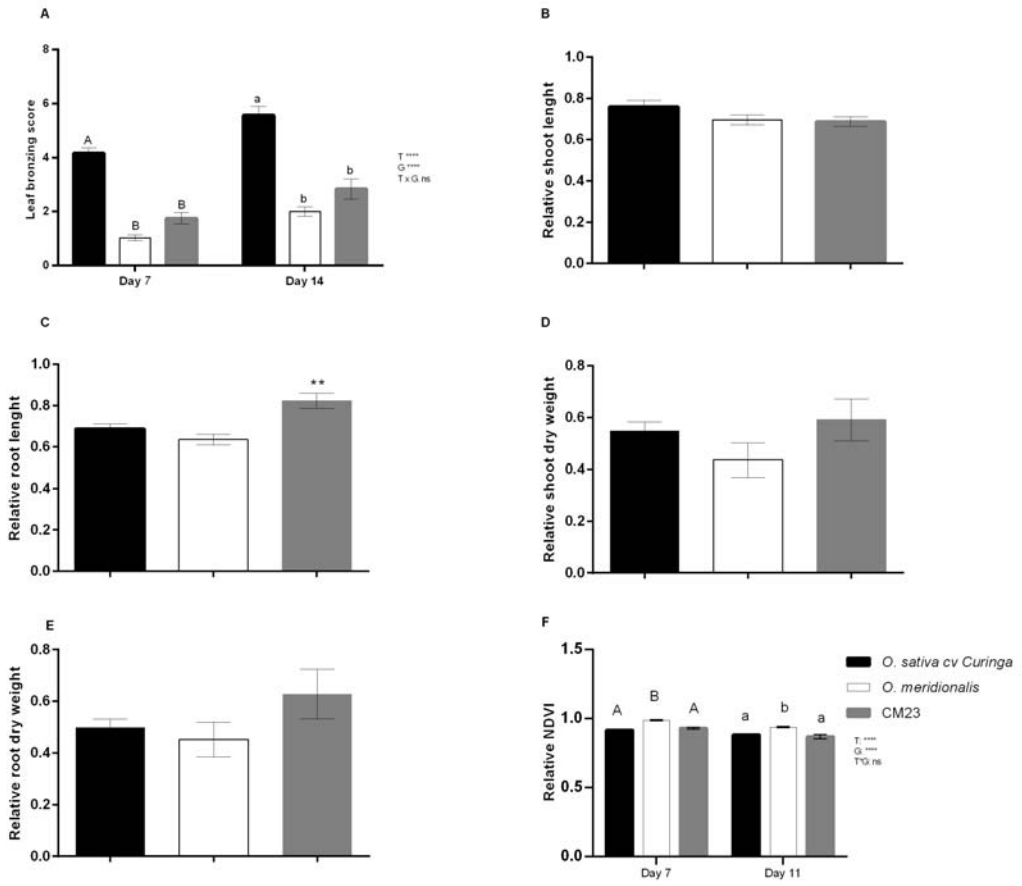

977

978

979 Figure 3

980

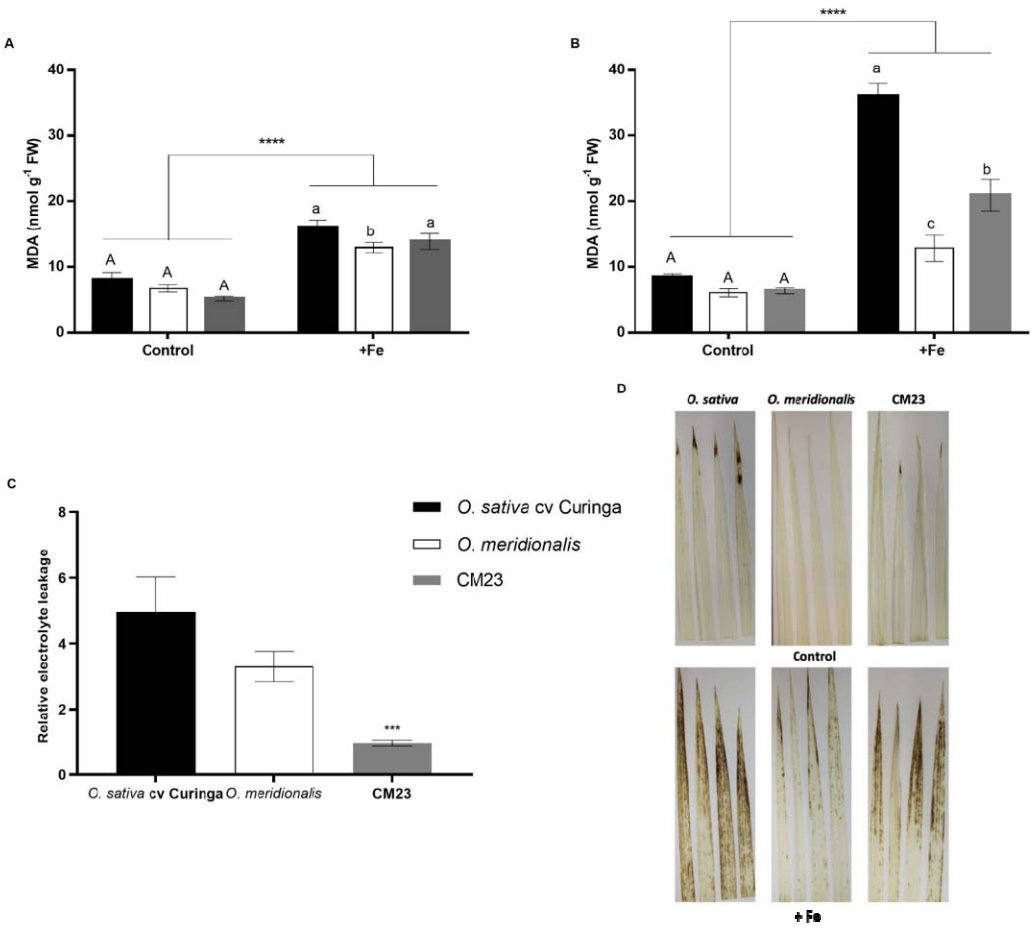

981

982

983 Figure 4

984

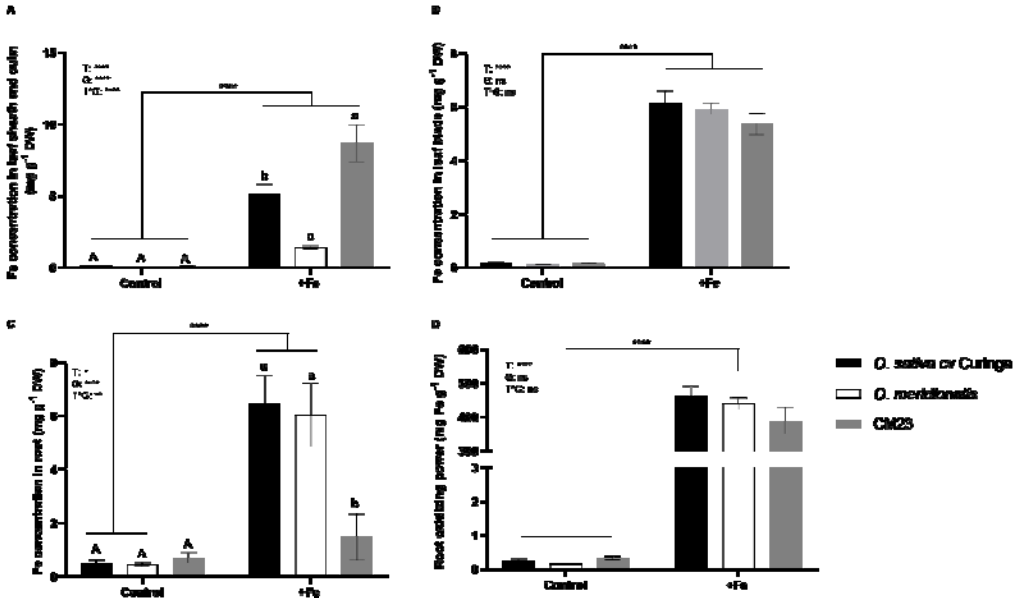

985

986

987 Figure 5

988

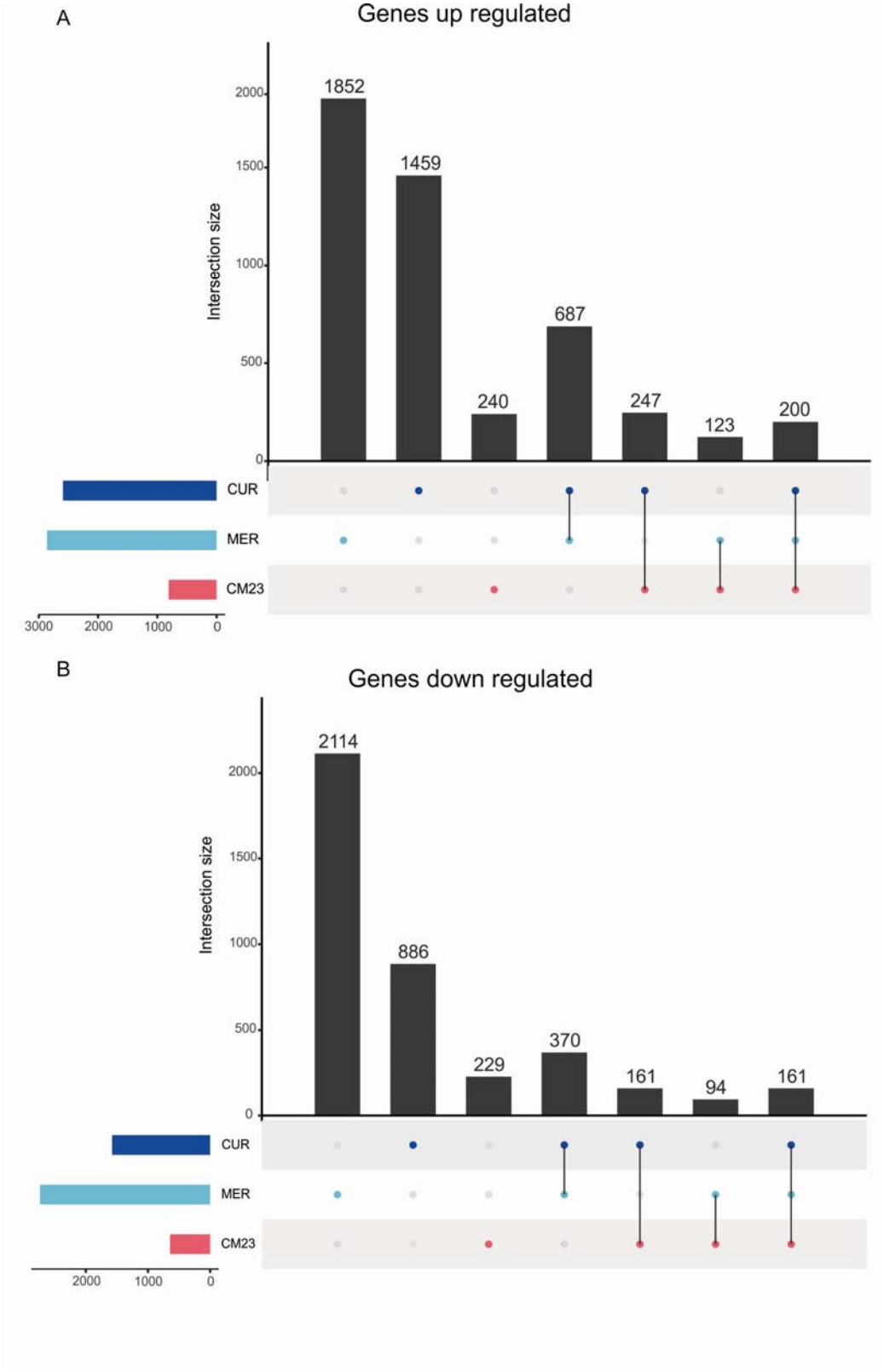

989

990 Figure 6

991

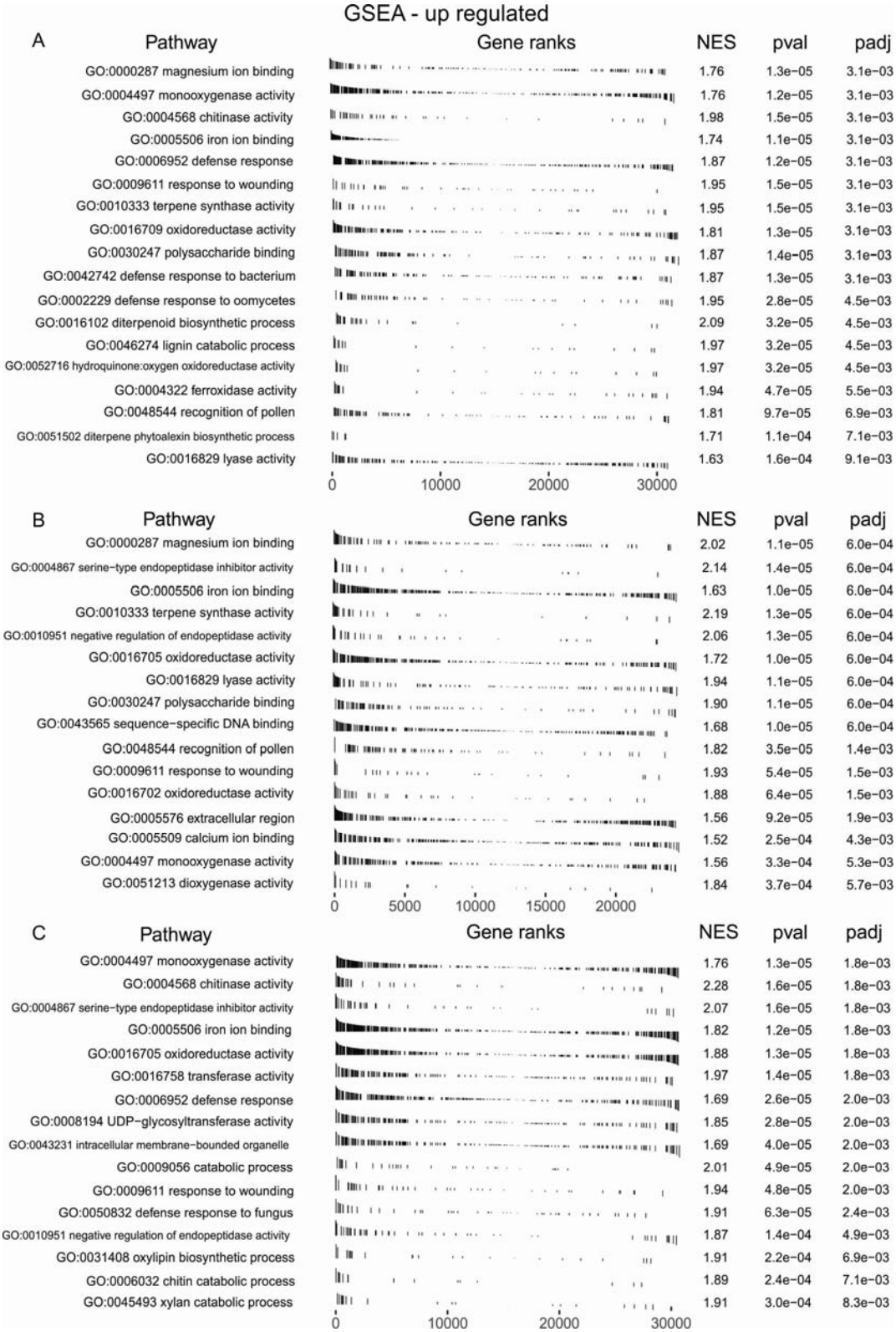

992

993

994 Figure 7

995

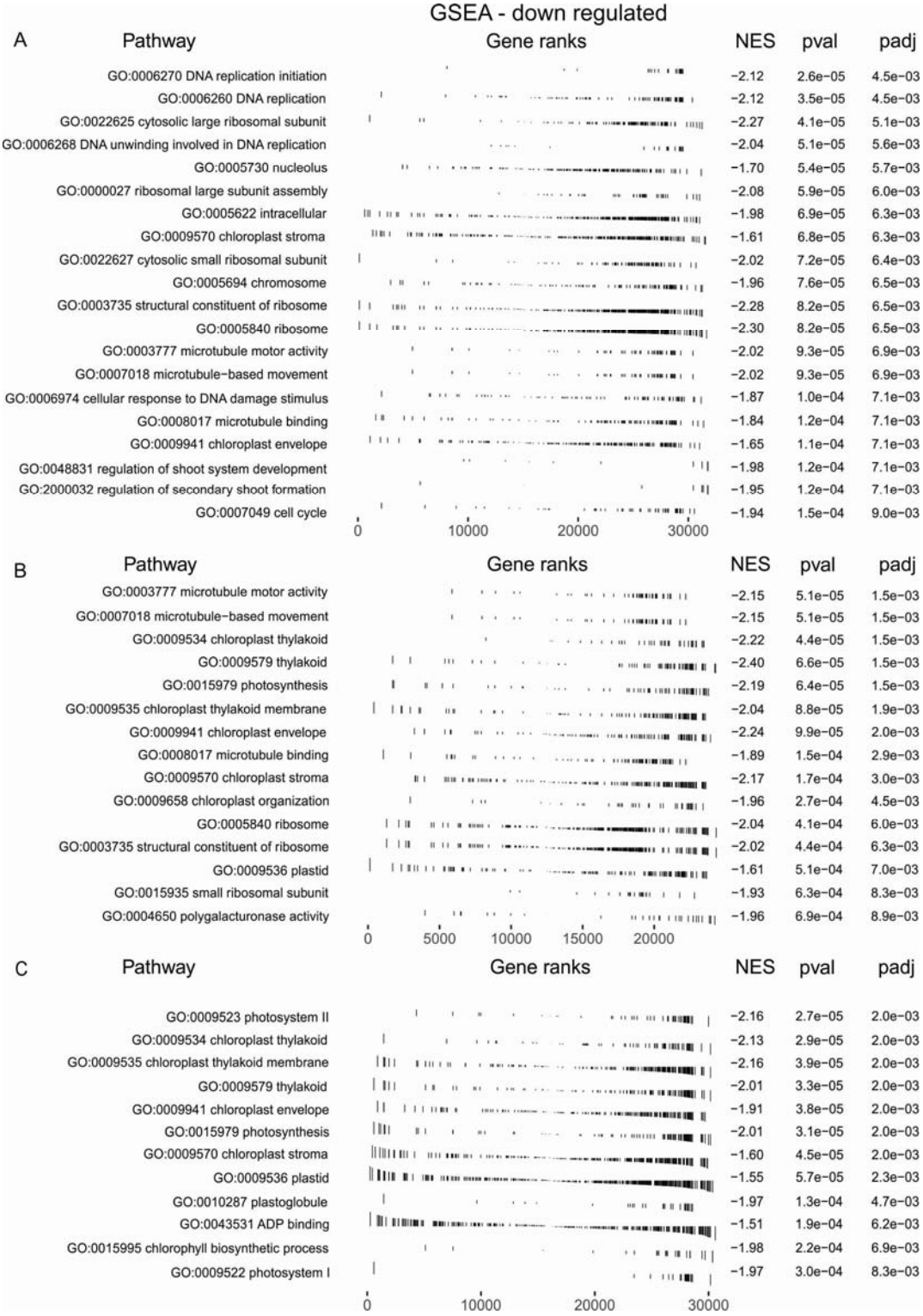

996

997